Neuron 49, 175–182, January 19, 2006 ©2006 Elsevier Inc. DOI 10.1016/j.neuron.2005.12.017

Report

A Critical Role for Myosin IIB in Dendritic Spine Morphology and Synaptic Function

Jubin Ryu,[1] Lidong Liu,[2] Tak Pan Wong,[2] Dong Chuan Wu,[2] Alain Burette,[3] Richard Weinberg,[3] Yu Tian Wang,[2] and Morgan Sheng[1,*]

[1] The Picower Institute for Learning and Memory
RIKEN-MIT Neuroscience Research Center
Howard Hughes Medical Institute
Massachusetts Institute of Technology
Cambridge, Massachusetts 02139

[2] Brain Research Centre
University of British Columbia
2211 Wesbrook Mall
Vancouver, British Columbia V6T 2B5
Canada

[3] Department of Cell and Developmental Biology
University of North Carolina
CB #7090
Chapel Hill, North Carolina 27599

Summary

Dendritic spines show rapid motility and plastic morphology, which may mediate information storage in the brain. It is presently believed that polymerization/depolymerization of actin is the primary determinant of spine motility and morphogenesis. Here, we show that myosin IIB, a molecular motor that binds and contracts actin filaments, is essential for normal spine morphology and dynamics and represents a distinct biophysical pathway to control spine size and shape. Myosin IIB is enriched in the postsynaptic density (PSD) of neurons. Pharmacologic or genetic inhibition of myosin IIB alters protrusive motility of spines, destabilizes their classical mushroom-head morphology, and impairs excitatory synaptic transmission. Thus, the structure and function of spines is regulated by an actin-based motor in addition to the polymerization state of actin.

Introduction

Dendritic spines are small protrusions that serve as the main site of excitatory synapses in the mammalian brain (Harris and Kater, 1994; Hering and Sheng, 2001). Spines exist in a variety of shapes and sizes, making them attractive structural candidates for learning and memory (Yuste and Bonhoeffer, 2001). In support of this idea, long-term potentiation (LTP) has been associated with increased spinogenesis and spine head growth, whereas long-term depression (LTD) has been associated with spine shrinkage and retraction (Engert and Bonhoeffer, 1999; Maletic-Savatic et al., 1999; Matsuzaki et al., 2001, 2004; Nagerl et al., 2004; Zhou et al., 2004).

In addition to their morphological plasticity, spines also display rapid motility, changing shape and size over seconds to minutes in dissociated culture, slice, and in vivo contexts (Fischer et al., 1998; Dunaevsky et al., 1999; Lendvai et al., 2000). These changes include the appearance and disappearance of filopodia, "amorphous" fluctuations of the spine head, elongation of the spine neck, emergence of filopodia from the spine head, and transient "kissing" of spine heads. These phenomena are thought to be important in synaptogenesis as well as in modulation of extant synapses (Bonhoeffer and Yuste, 2002).

It is widely believed that both the heterogeneous morphology and rapid motility of dendritic spines are determined by the polymerization and depolymerization of actin (Fischer et al., 1998; Hering and Sheng, 2001; Bonhoeffer and Yuste, 2002; Star et al., 2002; Ackermann and Matus, 2003; Okamoto et al., 2004). In other cell-biological contexts, however, actin dynamics are also regulated via a distinct and equally prominent mechanism: myosin motors. The myosin superfamily is characterized by the ability to bind actin and hydrolyze ATP in order to translocate and maintain tension in actin filaments (Sellers, 2000). Myosin II, a canonical member of this family, is a hexameric polypeptide comprised of two heavy chains and two pairs of regulatory light chains. In vertebrates, myosin II is typically divided into two classes: sarcomeric myosin II from skeletal muscle and nonmuscle myosin II. Nonmuscle myosin II, in turn, exists in two isoforms, A and B. While most tissues express equal amounts of both isoforms, neuronal tissue and embryonic cardiomyocytes express predominantly the B isoform (Kawamoto and Adelstein, 1991).

Nonmuscle myosin IIB (hereafter referred to as myosin IIB) is required for cytokinesis and maintenance of cortical tension in *Dictyostelium*, dorsal closure in *D. melanogaster*, maintenance of embryonic polarity in *C. elegans*, and neuronal migration and growth cone motility in mice (De Lozanne and Spudich, 1987; Young et al., 1993; Guo and Kemphues, 1996; Tullio et al., 1997). Recent studies have revealed additional unexpected roles for myosin IIB in mitotic spindle assembly and in cell intercalation during development of the *Drosophila* embryo (Rosenblatt et al., 2004; Bertet et al., 2004).

Proteomic analyses have uncovered the abundant presence of the heavy chain of myosin IIB (MHCIIB) in the postsynaptic density (PSD) fraction of rat brain (Jordan et al., 2004; Peng et al., 2004). In this study, we provide evidence that postsynaptic myosin IIB represents a means of regulating spine dynamics that is mechanistically distinct from actin polymerization/depolymerization. We report the subcellular distribution of myosin IIB in neurons and elucidate the function of myosin IIB by pharmacological inhibition and molecular genetic suppression with RNA interference (RNAi). Our data indicate a critical role for myosin IIB in the morphological integrity of dendritic spines and in the maintenance of synaptic transmission.

Results

To determine whether myosin IIB is enriched in the PSD, we surveyed its abundance in subcellular fractions of rat

*Correspondence: msheng@mit.edu

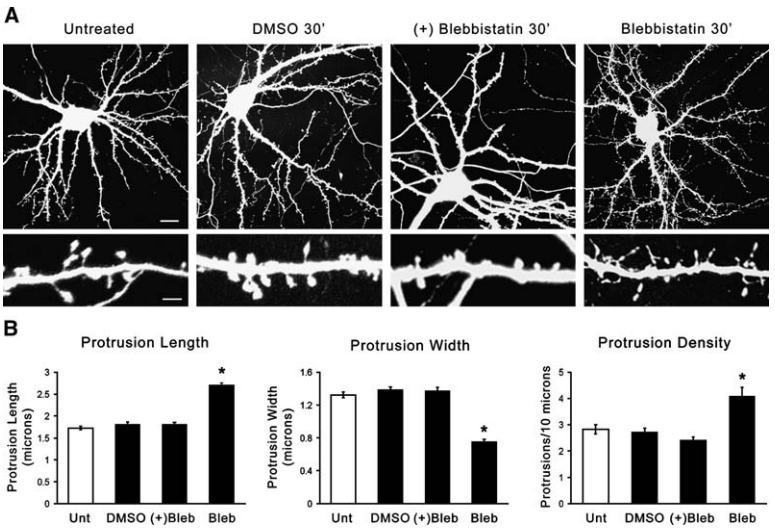

Figure 1. Blebbistatin Induces Loss of Mushroom Spines and Formation of Filopodia-like Protrusions

(A) DIV10 rat hippocampal neurons were transfected with β-gal. Seven days later, they were treated with nothing, DMSO, (+)blebbistatin (100 μM), or blebbistatin (100 μM) for 30 min, and fixed and immunostained for β-gal. Scale bar, 10 μm (low magnification); 2 μm (high-magnification image of dendrite). (B) Quantitation of protrusion length, width, and density in neurons treated with blebbistatin versus controls. *$p < 0.001$ cf. untreated neurons. Data represent mean ± SEM.

forebrain by immunoblotting (see Figure S1A in the Supplemental Data available online). Myosin IIB was significantly enriched in PSD fractions relative to crude synaptosomal fraction (P2), albeit to a lesser degree than the NMDA receptor subunit NR2A, an established PSD "marker" protein (Figure S1A). Like NR2A, myosin IIB was also abundant in P2 and P3 (light membrane) fractions, suggesting partial association with membranes.

To investigate the subcellular distribution of myosin IIB at the morphological level, we performed immunocytochemistry on rat hippocampal neurons in dissociated culture. In immature neurons (DIV8), myosin IIB immunoreactivity was present throughout the neuron but was more concentrated in the cell body and proximal dendrites (Figure S1B). In addition, myosin IIB staining was more intense at dendritic branch points and at the tips of dendrites and axons.

In more mature neurons (DIV18), myosin IIB diminished in the soma and localized primarily to dendrites, where it accumulated in a punctate pattern on top of a less intense diffuse staining (Figure S1C). Greater than 90% of myosin IIB dendritic puncta colocalized with the PSD marker PSD-95, consistent with a clustering of myosin IIB at synaptic sites. In addition, in roughly half of these colocalizations, the myosin IIB puncta was larger in size and extended past the PSD-95 margin toward the dendritic shaft (Figure S1C). Therefore, the zone of myosin IIB enrichment may extend past the spine head into the neck of the spine.

To examine myosin IIB localization in vivo, we immunostained hippocampal sections from ~90-day-old rats. Dense punctate labeling for myosin IIB filled the apical and basal dendritic fields of the CA1 region but was largely absent from the pyramidal cell soma (Figure S1D). The myosin IIB immunostaining showed extensive overlap with synaptophysin, a synaptic vesicle protein. Overall, the immunocytochemistry results are consistent with the biochemical fractionation data and support the idea that myosin IIB is enriched in but not exclusively localized to the postsynaptic compartment.

What is the function of myosin IIB in neurons? To address this question, we utilized blebbistatin, a recently discovered small molecule inhibitor of myosin II (Straight et al., 2003; Kovacs et al., 2004; Limouze et al., 2004). Blebbistatin specifically inhibits the ATPase activity of myosin II, trapping it in an ADP-bound state that has low affinity for actin. At DIV17, control neurons treated for 30 min with nothing, DMSO, or the inactive (+) enantiomer of blebbistatin exhibited mostly mushroom-shaped spines (Figure 1A). Neurons treated with active blebbistatin (100 μM, 30 min) lost most of their mushroom-headed spines and instead displayed long, thin filopodia-like processes that lacked heads (Figure 1A). Accordingly, quantitative morphometry showed an increase in mean length and a reduction in mean width of dendritic protrusions (Figure 1B). The density of protrusions per length of dendrite was also increased by blebbistatin, relative to controls treated with nothing, DMSO, or (+)blebbistatin (Figure 1B). In contrast to its effect on protrusion morphology, 100 μM blebbistatin did not alter cell soma circumference, dendrite length, or dendrite width (data not shown). In summary, pharmacological inhibition suggests that myosin IIB function is required over the timeframe of minutes to maintain the proper morphology of mature spines.

To confirm the veracity and specificity of the blebbistatin effect, we used a molecular genetic approach (RNAi) to suppress endogenous myosin IIB. Hippocampal neurons transfected at DIV14 for 6 days with a pSuper plasmid expressing small hairpin RNAs against rat myosin IIB showed loss of myosin IIB immunofluorescence (cell body intensity reduced to 30% of cell body intensity in neighboring untransfected cells; Figures 2A and 2B). There was little change in myosin IIB immunoreactivity in neurons transfected with empty pSuper vector.

Myosin IIB-RNAi resulted in a spine phenotype similar to that induced by 30 min blebbistatin treatment—namely, a loss of mushroom-headed spines and a profusion of irregular filopodia-like protrusions (Figures 2A and 2B). Myosin IIB-RNAi caused an increase in mean length and a decrease in mean width of dendritic protrusions relative to control transfected neurons (Figure 2B). Unlike blebbistatin, however, RNAi-mediated inhibition of myosin IIB did not affect the density of protrusions significantly (Figure 2B). Myosin IIB RNAi did not alter

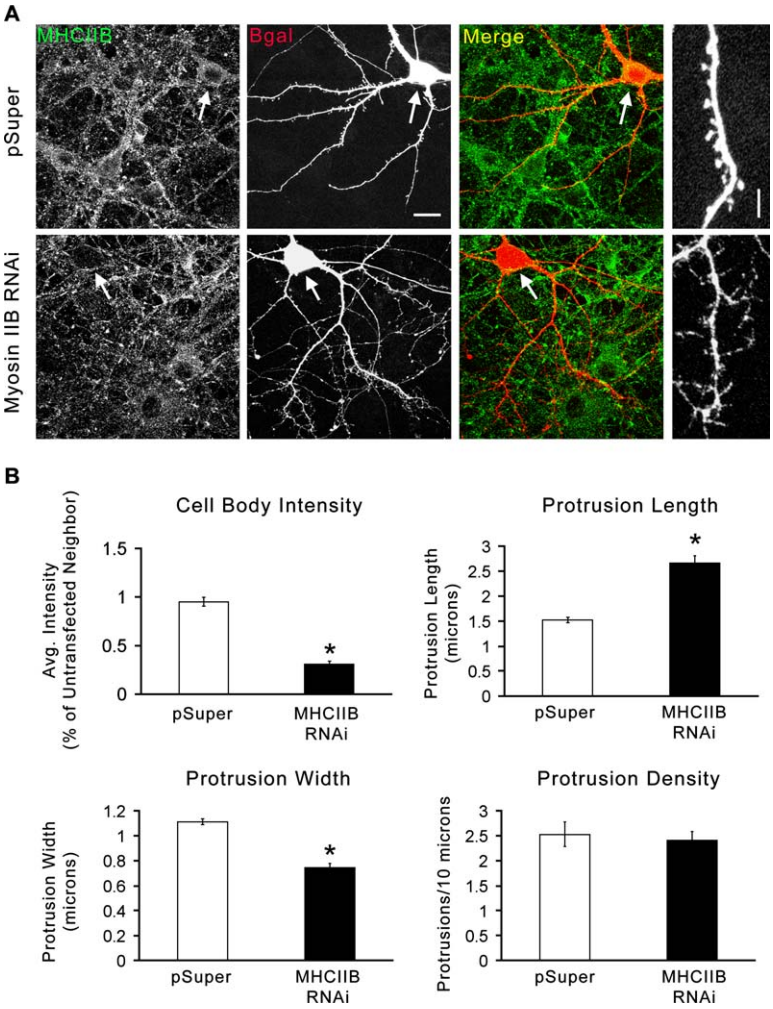

Figure 2. RNAi Knockdown of Myosin IIB Induces Loss of Mushroom Spines and Generation of Filopodia-like Protrusions

(A) DIV14 hippocampal neurons were transfected for 6 days with β-gal plus pSuper vector or myosin IIB-RNAi construct, as indicated, and stained for endogenous myosin IIB (green) and β-gal (red). Arrows indicate cell bodies of transfected cells. Rightmost panels show high-magnification views of individual transfected dendrites. Scale bar, 10 μm (low magnification) and 2 μm (high magnification). (B) Quantitation of myosin IIB immunofluorescence in the cell body, protrusion length, protrusion width, and protrusion density in transfected neurons. Myosin IIB staining intensity in the cell body was compared to untransfected neurons in the same field. *$p < 0.001$ cf. pSuper transfected neurons. Data represent mean ± SEM.

cell soma circumference, dendrite length, or dendrite width (data not shown). The overall similarity of the pharmacological and RNAi findings supports a specific role for myosin IIB in the maintenance of mushroom-headed spines in cultured neurons.

The above pharmacological and RNAi data imply that myosin IIB is required to maintain mushroom-headed spines while keeping filopodia in check, but this conclusion is based on examination of separate populations of fixed neurons. We therefore used time-lapse confocal imaging of live neurons to address the following question: does blebbistatin inhibition of myosin IIB cause mushroom spines to directly transform into filopodia-like protrusions, or are mushroom spines lost and subsequently replaced by new filopodia?

Over a 70 min period (imaged once per minute), control spines treated with DMSO (added at the eleventh minute) showed dynamic movements, as previously described (Dailey and Smith, 1996; Dunaevsky et al., 1999; Bonhoeffer and Yuste, 2002). Two major forms of motility were observed (Figure 3A and Movie S1). First, most spines fluctuated in overall shape without any apparent directionality ("amorphous motility") (Figure 3A, arrows). Second, some spines repeatedly extended and retracted filopodia-like projections from their head ("protrusive" motility) (Figure 3A, arrowheads). Despite the constant flux of these two types of motility, there was a general maintenance of spine dimensions over a timeframe of tens of minutes. During amorphous motility, the overall size of the spine remained the same despite the rapid "morphing" of the head. Each filopodial extension was almost always followed by a retraction that reeled it back in. Thus, control spines appeared much the same at the end of 70 min as they did at the start (Figure 3A, bottom).

Blebbistatin caused marked changes in shape, size, and motility of dendritic spines. During the 10 min prior to drug application, spines displayed typical amorphous and protrusive motility and retained their overall mushroom-head morphologies (Figure 3B and Movie S2). Following blebbistatin (added at the eleventh minute), spines adopted an altered protrusive motility. Rather than extend filopodial processes from their spine heads and then quickly retract them, blebbistatin-treated spines kept extending these projections without any retraction, resulting in long thin processes extending from the spine head (Figure 3B, arrowheads). Blebbistatin also caused a new behavior. Rather than "morphing" around a stable baseline size, many mushroom heads simply unfurled completely and transformed directly into a filopodium (Figure 3B, arrows). After 70 min of elapsed time, most of the original mushroom-shaped

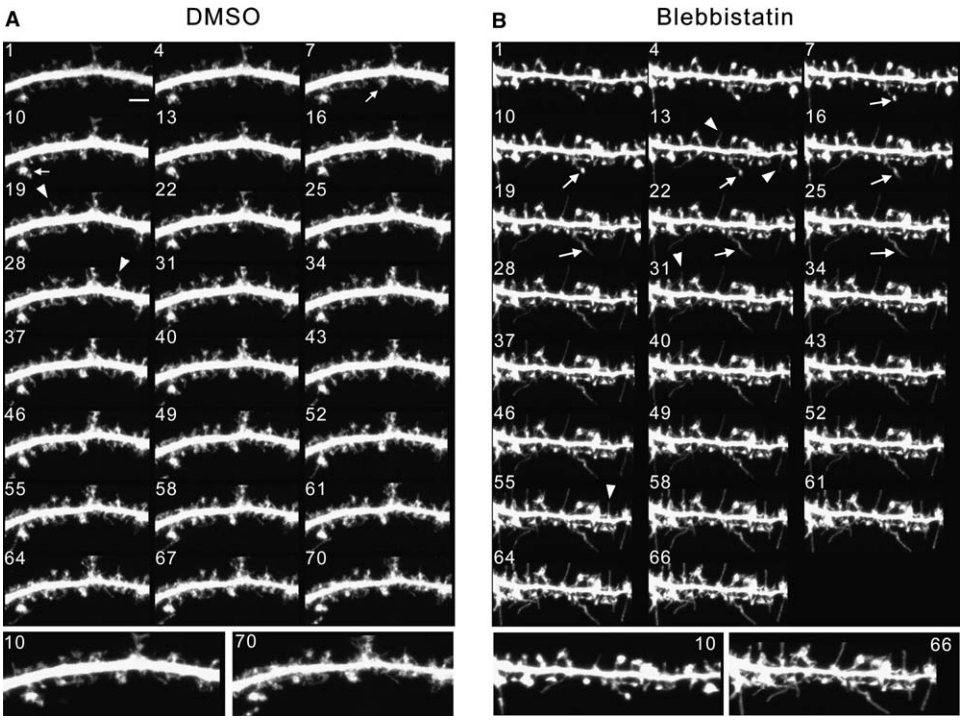

Figure 3. Time-Lapse Imaging of Blebbistatin Effects on Dendritic Spines

(A and B) DIV10 neurons were transfected with dsRed for 7 days and then imaged on DIV17. Images were captured every minute. Timestamp shows elapsed time in minutes (not all images are shown). In the first 10 min, neurons were left untreated. 100 μM blebbistatin (B) or DMSO (A) was added at 11 min. Arrows indicate examples of "amorphous" motility in DMSO-treated neurons (A), and examples of unfurling of dendritic spines into filopodia in blebbistatin-treated neurons (B). Arrowheads point to examples of filopodial extension/retraction in DMSO treated neurons (A), and to filopodial extension from spine heads in blebbistatin-treated neurons (B). Scale bar, 2 μm. Bottom panels show higher-magnification views of early and late time points (time stamp in minutes).

spines showed completely changed morphology, either with long filopodia-like protrusions extending from their heads or being transformed into a filopodium (Figure 3B, bottom). Time-lapse imaging revealed that filopodia arose directly from spines, rather than de novo.

Given its role in the maintenance of dendritic spine morphology, myosin IIB might be important for the integrity of the synapse. We tested this by immunostaining for surface AMPA receptors in DIV17 dissociated hippocampal neurons after 30 min treatment with 100 μM blebbistatin. Compared to control neurons treated with DMSO, blebbistatin-treated neurons showed a reduction in linear density of AMPAR puncta, and those puncta that remained were larger in size and irregularly shaped (Figure S2). Parallel immunostaining experiments showed no change in puncta density and size of the presynaptic marker Bassoon following blebbistatin treatment (30 min, 100 μM) (Figure S2). These findings suggest that blebbistatin primarily affects synapse structure on the postsynaptic side.

To examine a potential role for myosin IIB in synaptic transmission, we tested the effects of blebbistatin on AMPA receptor-mediated EPSCs recorded from CA1 neurons in acute rat hippocampal slices in response to stimulation of Schaffer collateral inputs. In order to expose only postsynaptic cells to the drug, we applied blebbistatin (50 μM) to CA1 neurons intracellularly via the recording pipette. Starting ~10 min after "break-in," blebbistatin caused a progressive decrease in amplitude of EPSCs. Synaptic responses were depressed to ~60% after 60 min exposure to the drug (Figures 4A and 4B). Control neurons exposed to normal intracellular solution, DMSO, or (+)blebbistatin in the recording pipette maintained their AMPA-EPSCs over the same timecourse (Figures 4A and 4B).

We also tested the effects of blebbistatin on mini-EPSCs in dissociated hippocampal neurons. Neurons filled intracellularly with 50 μM blebbistatin through the recording pipette displayed a 36% decrease in frequency and 27% decrease in amplitude of mini-EPSCs after 50 min (Figures 4C and 4D). Neurons treated with DMSO or (+)blebbistatin showed no change in frequency or amplitude of mini-EPSCs.

Discussion

Spine morphology and motility are believed to be regulated primarily by dynamic polymerization and depolymerization of the actin cytoskeleton. In support of this, pharmacologic inhibition of actin polymerization with cytochalasin-D inhibits spine motility in both dissociated and slice cultures (Fischer et al., 1998; Dunaevsky et al., 1999). In addition, the F-actin/G-actin ratio and actin turnover in spines are regulated by activity (Star et al., 2002; Okamoto et al., 2004).

A role for actomyosin contraction in spine dynamics was initially excluded, based on pharmacological inhibition using 2,3 butanedione-monoxime (BDM); these

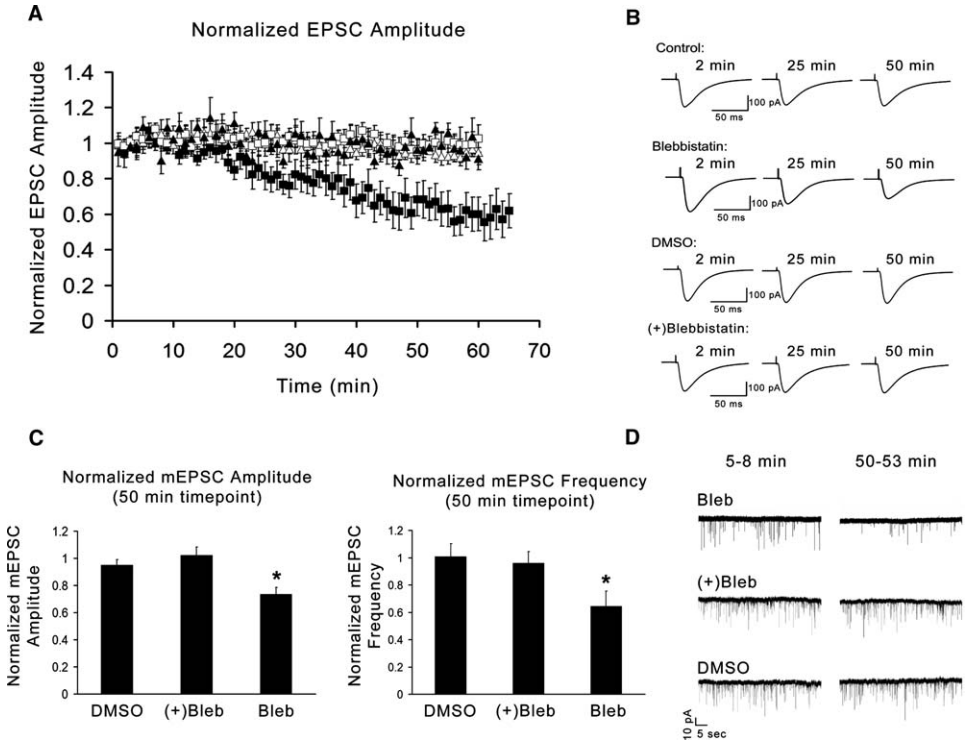

Figure 4. Inhibition of Excitatory Synaptic Transmission by Blebbistatin

(A) Blebbistatin (50 μM) was administered intracellularly via the recording pipette in CA1 pyramidal neurons of acute hippocampal slices, and AMPA receptor-mediated EPSCs were recorded following Schaffer collateral stimulation (filled squares). Control slices were recorded with normal intracellular solution (open triangles), 0.1% DMSO (open squares), or 50 μM (+)blebbistatin (filled triangles) in the pipette. EPSC amplitude was normalized to baseline. Data represent mean ± SEM. (B) Representative EPSC traces from neurons treated with normal intracellular solution, DMSO, (+)blebbistatin, or active blebbistatin. Traces were averaged from 5 min of uninterrupted recording begun at indicated time points. (C) Blebbistatin (50 μM) was administered intracellularly via the recording pipette into dissociated rat hippocampal neurons (DIV12–14), and mini-EPSCs were recorded over 50 min. Control neurons were filled with either DMSO or 50 μM (+)blebbistatin. Mean amplitude and frequency of mEPSCs recorded from 50–53 min after patching were normalized to mean mEPSC amplitude and frequency from 5–8 min. *$p < 0.05$ cf. 5 min time point. Data represent mean ± SEM. (D) Representative mEPSC recordings from dissociated hippocampal neurons filled intracellularly with DMSO, (+)blebbistatin and active blebbistatin. Recordings are from 5–8 min after patching and from 50–53 min after patching.

experiments showed no effect on morphology or motility of spines after drug treatment (Fischer et al., 1998). BDM, however, was found in subsequent years to be a poor inhibitor for several reasons. First, it has only a low affinity for skeletal myosin II (K_I ~5 mM), and against nonmuscle myosin II, it has no detectable inhibitory activity (Cramer and Mitchison, 1995; Cheung et al., 2002). In addition, BDM nonspecifically affects other proteins in the cell, including myosin II light chain kinase, connexins, potassium channels, and L-type calcium channels (Ostap, 2002). In terms of affinity and specificity for nonmuscle myosin II, the recently discovered inhibitor blebbistatin appears to represent an improvement over BDM. Blebbistatin has a K_I of ~2 μM, and at 50 μM, inhibits both myosin IIA and IIB to ~10% of their maximal ATPase activity. In addition, blebbistatin does not inhibit myosins I, V, or X (Straight et al., 2003).

In light of recent mass spectrometry data showing an abundance of myosin heavy chain IIB in the PSD, we sought to re-examine a potential role for this molecular motor in spine dynamics (Jordan et al., 2004; Peng et al., 2004). The enrichment of myosin IIB in the PSD fraction and its immunocytochemical localization at synapses is consistent with a role for this molecular motor in shaping the dendritic spine head. In addition to its favorable position at synaptic sites, loss-of-function experiments—both pharmacologic and genetic—showed that myosin IIB is in fact essential for spine morphology and normal motility. Both blebbistatin and myosin IIB-RNAi led to depletion of mushroom-type spines and their replacement with irregular filopodia-like processes. The action of blebbistatin is rapid, with time-lapse studies revealing profound alterations in spine morphology and motility occurring within tens of minutes of drug application. Blebbistatin-induced inhibition of myosin IIB also appears to have functional consequences, resulting in a depression of EPSCs and a decrease in both frequency and amplitude of mini-EPSCs; these effects are more likely secondary to the disruption of synaptic architecture rather than reflecting a direct role of myosin IIB in synaptic transmission.

Blebbistatin can inhibit both myosin IIA and -B, and its neuronal effects could hypothetically be due to inhibition of either or both. We believe that inhibition of myosin IIB most likely underlies the observed phenotype because the IIB isoform is expressed at higher levels in neurons than IIA (Kawamoto and Adelstein, 1991; data not shown), and because RNAi of myosin IIB alone increases protrusion length and decreases protrusion width, similarly to blebbistatin. Nevertheless, it should

be noted that our study does not rule out a role for myosin IIA in regulation of spine morphology.

In many other cellular contexts, myosin IIB serves to contract or maintain tension in actin filament networks. For example, this contractile function is required for cytokinesis as well as cortical tension in *Dictyostelium* (Knecht and Loomis, 1987; Pasternak et al., 1989). In *Saccharomyces cerevisiae,* ablation of myosin II results in aberrant cell wall formation at the mother/bud neck, disrupting cell division (Watts et al., 1987). How do these well-conserved functions shed light on the dendritic spine phenotypes caused by myosin IIB loss of function? The volatile projection of filopodia from spine heads could be explained if myosin IIB is required to maintain the integrity of the mushroom surface by generating tangential forces at the spine head membrane. This "surface tension" could counteract the forces of polymerizing actin that act outwardly in a perpendicular direction to the membrane surface to extend filopodia. The unraveling of a mushroom into a filopodium, in turn, could be a more severe consequence of the loss of tangential surface tension in the bulbous spine head. Further studies need to be performed to precisely describe where and how myosin IIB is acting biophysically.

As a regulator of spine morphology and motility, myosin IIB possesses attractive properties. Its actin binding activity is highly regulated, primarily by phosphorylation of the Ser19 residue on its regulatory light chain, and this light chain has been shown to bind directly to the C termini of the NR1 and NR2 subunits of NMDA receptors (Suzuki et al., 1978; Amparan et al., 2005). The phosphorylation state of myosin light chain is controlled by signaling pathways that are prominent in neurons and in the PSD in particular. For example, myosin light chain kinase (MLCK), which phosphorylates and thereby activates myosin IIB, is stimulated by Ca^{2+}/calmodulin (Goeckeler and Wysolmerski, 1995). In addition, P21-associated kinase (PAK), and Rho-associated kinase (ROCK) have been shown to directly phosphorylate myosin IIB (Chew et al., 1998; Amano et al., 1998) and to regulate spine morphology (Hayashi et al., 2004).

ROCK is particularly compelling because it is a primary effector of RhoA, a small GTPase with profound consequences on neuronal and spine morphology. Constitutively active RhoA results in marked loss of dendritic spines when transfected into rat hippocampal slices (Nakayama et al., 2000), and this phenotype could perhaps be explained in part by a Rho-ROCK-myosin cascade, culminating in myosin contraction of actin filaments and retraction of spines. Such a model is admittedly simplistic, as Rho and ROCK can influence other proteins as well. In growth cones of retinal ganglion neurons, for example, ROCK regulates filopodial extension via ADF/cofilin rather than myosin IIB, suggesting that the reduction of spines caused by active RhoA could be mediated by inhibition of ADF/cofilin as well as through myosin IIB activation (Gehler et al., 2004).

In conclusion, our findings suggest that spine morphology and motility are not controlled solely by actin polymerization/depolymerization, but are also critically dependent on the molecular motor myosin IIB. Because it can reversibly bind and contract actin, and because it can be bidirectionally regulated, myosin IIB appears to be a novel and potent means of controlling the dynamic structure of dendritic spines.

Experimental Procedures

Antibodies and Drugs

The following antibodies have been described previously: rabbit NR2A (Sheng et al., 1994) and monoclonal PSD95 (Hering and Sheng, 2003). The following antibodies were purchased commercially: MHCIIB (Covance, Berkeley, CA); β-galactosidase (Promega, Madison, WI); GluR1 (Calbiochem, Darmstadt, Germany); Bassoon (StressGen, Sidney, Canada). Blebbistatin was purchased from Tocris (Ellisville, MO).

DNA Constructs

The following oligonucleotides (targeted to nts 4362-4380 of rat MHCIIB) were annealed and cloned into pSuper vector to make the RNAi construct against MHCIIB: 5′-gatccccgaagccaagaagaa actgcttcaagagagcagtttcttcttggcttctttttggaaa-3′ and 5′-agctttccaaa aagaagccaagaagaaactgctctcttgaagcagtttcttcttggcttcggg-3′. mRFP was cloned into pGWI vector. DsRed2 expression plasmid was from Clontech.

Subcellular and PSD Fractionation

Two adult rat forebrains were fractionated as described (Huttner et al., 1983). Forebrains were homogenized and spun at 1400 × g, and the supernatant (S1) was set aside. The pellet (P1) was homogenized and spun at 710 × g. The supernatant was pooled with S1and spun at 13,800 × g. The supernatant (S2) was set aside. The pellet (P2) was layered onto a discontinuous sucrose gradient and spun at 82,500 × g. The synaptosomal fraction was isolated from the 1.0/1.2 M sucrose interface and spun at 32,800 × g, and the pellet (PSDI) was resuspended. PSDII and -III were obtained by Triton and Sarcosyl extractions of the PSDI pellet, respectively. These pellets were spun down at 201,800 × g. S2 was also spun down at this stage to produce S3 and P3.

Neuronal Culture, Immunostaining, Drug Treatment, and Transfection

Hippocampal neurons were dissected from E20 Sprague-Dawley rat embryos, plated onto coated glass coverslips (30 μg/mL PDL and 2.5 μg/mL laminin), and cultured in Neurobasal medium (Invitrogen) with B27 (Invitrogen), 0.5 mM glutamine, and 12.5 μM glutamate.

For MHCIIB, PSD95, and Bassoon staining, neurons were fixed in 100% methanol for 10 min at −20ºC. Neurons in the blebbistatin trials were fixed in 4% PFA/4% sucrose at RT for 10 min. RNAi transfected neurons were fixed in 4% PFA/4% sucrose for 3 min at RT, followed by 10 min in 100% methanol at −20ºC. For AMPAR staining, neurons were incubated in GluR1 antibody (diluted in DMEM) at 37ºC for 10 min and fixed in 4% PFA/4% sucrose for 8 min at RT. Immunostaining was performed as previously described (Sala et al., 2001). Blebbistatin was administered to neurons by diluting 50 mM stock 1:500 into conditioned neuron media, for a final concentration of 100 μM. All transfections were done using calcium phosphate (Sala et al., 2001). For the blebbistatin trials, neurons were transfected with 4 μg β-gal/well. For RNAi experiments, each well of neurons was cotransfected with 2.5 μg of β-gal and 7.5 μg of pSuper or MHCIIB RNAi.

Microscopy and Quantitation

Fixed neurons were imaged with an LSM510 confocal microscope system (Zeiss, Oberkochen, Germany) and an Axioplan microscope (Zeiss). A 63× oil-immersion lens (N.A. 1.40) was used. Except for neurons costained for PSD95 and MHCIIB, each image consisted of a z-stack projected into one image. Live imaging was performed using Multi-time software (Zeiss) with a Pascal confocal system (Zeiss) and an Axiovert microscope (Zeiss), using a 100× oil immersion lens and ~3.5× digital zoom. Cells were treated with 10 mM HEPES (pH 7.4) and imaged at 37ºC/5% CO_2.

Morphometric measurements were performed using MetaMorph Software (Universal Imaging, West Chester, PA). For colocalization quantification, the PSD95 and MHCIIB channels were parsed into

separate images. A threshold level for each channel was manually set in order to exclude diffuse background staining, leaving only the puncta visible; the same threshold level was used for each neuron. The two thresholded images—each in a different color—were overlaid upon each other and the percentage of puncta overlapping with each other was manually counted. Ten neurons were used for this analysis.

In the blebbistatin experiments, 10 to 15 neurons were imaged for each of the four conditions. For each neuron, five 50–70 μm dendritic segments were chosen for spine morphometric analysis. Protrusions were defined as being >0.5 μm in length. Protrusion length was defined as the distance from the base to the tip of the protrusion; width was defined as the maximum distance perpendicular to the long axis of the protrusion. For each neuron, all the spine length, width, and density values were averaged into a single value; each cell was represented by one spine length, width, and density. The values for all neurons within a condition were then used to calculate a mean and SEM. For the RNAi experiments, 10 to 15 neurons were imaged for pSuper and MHCIIB RNAi transfected neurons. The cell soma was manually traced using the immunofluorescence of the transfected marker βgal; a projection constructed from a stack of confocal images was used for each neuron. Once the tracing was finished, the average intensity of the traced area was quantified in the MHCIIB channel. Cell body immunofluorescence was quantified by comparing the average intensity of the transfected neuron's cell soma to the soma of an untransfected neighbor in the same visual field. Spine morphometric analysis in the RNAi experiments was performed in the same manner as in the blebbistatin experiments. For AMPAR-mediated EPSC experiments, 6 to 12 neurons were used for each condition. For mEPSC experiments, 5 to 7 neurons were used for each condition.

Electrophysiology

Hippocampal slices were prepared from 19- to 23-day-old Sprague-Dawley rats. 400 μm coronal brain slices were cut using a vibrating blade microtome in ice-cold ACSF containing (in mM) 126 NaCl, 2.5 KCl, 1 $MgCl_2$, 1 $CaCl_2$, 1.25 KH_2PO_4, 26 $NaHCO_3$, and 20 glucose that was bubbled with 95% O_2/5% CO_2. Slices were recovered at 34ºC for 1.5 hr and maintained at RT. Slices were perfused at RT with carbogenated ACSF during recording. Whole-cell recordings of CA1 neurons were performed with a MultiClamp 700A amplifier (Axon Instruments, Foster City, CA) at holding potential –60 mV. The recording pipettes (6–8 MΩ) were filled with pH 7.2 solution containing (in mM) 132.5 Cs-gluconate, 17.5 CsCl, 2 $MgCl_2$, 0.5 EGTA, 10 HEPES, 4 ATP, and 5 QX-314. Cells were excluded if >20% change in the series or input resistance occurred. EPSCs were evoked every 20s by stimulating the Schaffer collateral-commissural pathway via a constant current pulse (0.05 ms) delivered in the presence of bicuculline methiodide (10 μM) in ACSF.

For mEPSCs, DIV12-14 cultured neurons were perfused with ECS containing (in mM) 140 NaCl, 5.4 KCl, 1 $MgCl_2$, 1.3 $CaCl_2$, 25 HEPES, and 30 glucose (pH 7.35), in addition to bicuculline (10 μM) and tetrodotoxin (0.5 μM). Whole-cell patch-clamp recordings were performed at a holding membrane potential of −60 mV with an AXOPATCH-1D amplifier (Axon). Recordings were low-pass filtered at 2 kHz, sampled at 10 kHz, and stored as data files using Clampex 8.0 (Axon). Recordings where the series resistance varied more than 10% were rejected.

Supplemental Data

The Supplemental Data for this article can be found online at http://www.neuron.org/cgi/content/full/49/2/175/DC1/.

Acknowledgments

M.S. is an investigator of the Howard Hughes Medical Institute.

Received: June 1, 2005
Revised: November 7, 2005
Accepted: December 9, 2005
Published: January 18, 2006

References

Ackermann, M., and Matus, A. (2003). Activity-induced targeting of profilin and stabilization of dendritic spine morphology. Nat. Neurosci. *6*, 1194–1200.

Amano, M., Chihara, K., Nakamura, N., Fukata, Y., Yano, T., Shibata, M., Ikebe, M., and Kaibuchi, K. (1998). Myosin II activation promotes neurite retraction during the action of Rho and Rho-kinase. Genes Cells *3*, 177–188.

Amparan, D., Avram, D., Thomas, C.G., Lindahl, M.G., Yang, J., Bajaj, G., and Ishmael, J.E. (2005). Direct interaction of myosin regulatory light chain with the NMDA receptor. J. Neurochem. *92*, 349–361.

Bertet, C., Sulak, L., and Lecuit, T. (2004). Myosin-dependent junction remodelling controls planar cell intercalation and axis elongation. Nature *429*, 667–671.

Bonhoeffer, T., and Yuste, R. (2002). Spine motility: phenomenology, mechanisms, and function. Neuron *35*, 1019–1027.

Cheung, A., Dantzig, J.A., Hollingworth, S., Baylor, S.M., Goldman, Y.E., Mitchison, T.J., and Straight, A.F. (2002). A small-molecule inhibitor of skeletal muscle myosin-II. Nat. Cell Biol. *4*, 83–88.

Chew, T.L., Masaracchia, R.A., Goeckeler, Z.M., and Wysolmerski, R.B. (1998). Phosphorylation of non-muscle myosin II regulatory light chain by p21-activated kinase (gamma-PAK). J. Muscle Res. Cell Motil. *19*, 839–854.

Cramer, L.P., and Mitchison, T.J. (1995). Myosin is involved in postmitotic cell spreading. J. Cell Biol. *131*, 179–189.

Dailey, M.E., and Smith, S.J. (1996). The dynamics of dendritic structure in developing hippocampal slices. J. Neurosci. *16*, 2983–2994.

De Lozanne, A., and Spudich, J.A. (1987). Disruption of the Dictyostelium myosin heavy chain gene by homologous recombination. Science *236*, 1086–1091.

Dunaevsky, A., Tashiro, A., Majewska, A., Mason, C.A., and Yuste, R. (1999). Developmental regulation of spine motility in mammalian CNS. Proc. Natl. Acad. Sci. USA *96*, 13438–13443.

Engert, F., and Bonhoeffer, T. (1999). Dendritic spine changes associated with hippocampal long-term synaptic plasticity. Nature *399*, 66–70.

Fischer, M., Kaech, S., Knutti, D., and Matus, A. (1998). Rapid actin-based plasticity in dendritic spines. Neuron *20*, 847–854.

Gehler, S., Shaw, A., Sarmier, P., Bamburg, J., and Letourneau, P. (2004). Brain-derived neurotrophic factor regulation of retinal growth cone filopodial dynamics is mediated through actin depolymerizing factor/cofilin. J. Neurosci. *24*, 10741–10749.

Goeckeler, Z.M., and Wysolmerski, R.B. (1995). Myosin light chain kinase regulated endothelial cell contraction—the relationship between isometric tension, actin polymerization and myosin phosphorylation. J. Cell Biol. *130*, 613–627.

Guo, S., and Kemphues, K.J. (1996). A non-muscle myosin required for embryonic polarity in Caenorhabditis elegans. Nature *382*, 455–458.

Harris, K.M., and Kater, S.B. (1994). Dendritic spines: cellular specializations imparting both stability and flexibility to synaptic function. Annu. Rev. Neurosci. *17*, 341–371.

Hayashi, M.L., Choi, S.Y., Rao, B.S., Jung, H.Y., Lee, H.K., Zhang, D., Chattarji, S., Kirkwood, A., and Tonegawa, S. (2004). Altered cortical synaptic morphology and impaired memory consolidation in forebrain-specific dominant-negative PAK transgenic mice. Neuron *43*, 773–787.

Hering, H., and Sheng, M. (2001). Dendritic spines: structure, dynamics and regulation. Nat. Rev. Neurosci. *2*, 880–888.

Hering, H., and Sheng, M. (2003). Activity-dependent redistribution and essential role of cortactin in dendritic spine morphogenesis. J. Neurosci. *23*, 11759–11769.

Huttner, W.B., Schiebler, W., Greengard, P., and De Camilli, P. (1983). Synapsin I (Protein I), a nerve terminal-specific phosphoprotein. III. Its association with synaptic vesicles studied in a highly purified synaptic vesicle preparation. J. Cell Biol. *96*, 1374–1388.

Jordan, B.A., Fernholz, B.D., Boussac, M., Xu, C., Grigorean, G., Ziff, E.B., and Neubert, T.A. (2004). Identification and verification of novel

rodent postsynaptic density proteins. Mol. Cell. Proteomics *3*, 857–871.

Kawamoto, S., and Adelstein, R.S. (1991). Chicken nonmuscle myosin heavy chains: differential expression of two mRNAs and evidence for two different polypeptides. J. Cell Biol. *112*, 915–924.

Knecht, D.A., and Loomis, W.F. (1987). Antisense RNA inactivation of myosin heavy chain gene expression in Dictyostelium discoideum. Science *236*, 1081–1086.

Kovacs, M., Toth, J., Hetenyi, C., Malnasi-Csizmadia, A., and Sellers, J.R. (2004). Mechanism of blebbistatin inhibition of myosin II. J. Biol. Chem. *279*, 35557–35563.

Lendvai, B., Stern, E., Chen, B., and Svoboda, K. (2000). Experience-dependent plasticity of dendritic spines in the developing rat barrel cortex in vivo. Nature *404*, 876–881.

Limouze, J., Straight, A.F., Mitchison, T., and Sellers, J.R. (2004). Specificity of blebbistatin, an inhibitor of myosin II. J. Muscle Res. Cell Motil. *25*, 337–341.

Maletic-Savatic, M., Malinow, R., and Svoboda, K. (1999). Rapid dendritic morphogenesis in CA1 hippocampal dendrites induced by synaptic activity. Science *283*, 123–127.

Matsuzaki, M., Ellis-Davies, G.C., Nemoto, T., Miyashita, Y., Iino, M., and Kasai, H. (2001). Dendritic spine geometry is critical for AMPA receptor expression in hippocampal CA1 pyramidal neurons. Nat. Neurosci. *4*, 1086–1092.

Matsuzaki, M., Honkura, N., Ellis-Davies, G.C., and Kasai, H. (2004). Structural basis of long-term potentiation in single dendritic spines. Nature *429*, 761–766.

Nagerl, U.V., Eberhorn, N., Cambridge, S., and Bonhoeffer, T. (2004). Bidirectional activity-dependent morphological plasticity in hippocampal neurons. Neuron *44*, 759–767.

Nakayama, A.Y., Harms, M.B., and Luo, L. (2000). Small GTPases Rac and Rho in the maintenance of dendritic spines and branches in hippocampal pyramidal neurons. J. Neurosci. *20*, 5329–5338.

Okamoto, K., Nagai, T., Miyawaki, A., and Hayashi, Y. (2004). Rapid and persistent modulation of actin dynamics regulates postsynaptic reorganization underlying bidirectional plasticity. Nat. Neurosci. *7*, 1104–1112.

Ostap, E.M. (2002). 2,3-Butanedione monoxime (BDM) as a myosin inhibitor. J. Muscle Res. Cell Motil. *23*, 305–308.

Pasternak, C., Spudich, J.A., and Elson, E.L. (1989). Capping of surface receptors and concomitant cortical tension are generated by conventional myosin. Nature *341*, 549–551.

Peng, J., Kim, M.J., Cheng, D., Duong, D.M., Gygi, S.P., and Sheng, M. (2004). Semiquantitative proteomic analysis of rat forebrain postsynaptic density fractions by mass spectrometry. J. Biol. Chem. *279*, 21003–21011.

Rosenblatt, J., Cramer, L.P., Baum, B., and McGee, K.M. (2004). Myosin II-dependent cortical movement is required for centrosome separation and positioning during mitotic spindle assembly. Cell *117*, 361–372.

Sala, C., Piech, V., Wilson, N.R., Passafaro, M., Liu, G., and Sheng, M. (2001). Regulation of dendritic spine morphology and synaptic function by Shank and Homer. Neuron *31*, 115–130.

Sellers, J.R. (2000). Myosins: a diverse superfamily. Biochim. Biophys. Acta *1496*, 3–22.

Sheng, M., Cummings, J., Roldan, L.A., Jan, Y.N., and Jan, L.Y. (1994). Changing subunit composition of heteromeric NMDA receptors during development of rat cortex. Nature *368*, 144–147.

Star, E.N., Kwiatkowski, D.J., and Murthy, V.N. (2002). Rapid turnover of actin in dendritic spines and its regulation by activity. Nat. Neurosci. *5*, 239–246.

Straight, A.F., Cheung, A., Limouze, J., Chen, I., Westwood, N.J., Sellers, J.R., and Mitchison, T.J. (2003). Dissecting temporal and spatial control of cytokinesis with a myosin II Inhibitor. Science *299*, 1743–1747.

Suzuki, H., Onishi, K., Takahashi, K., and Watanable, S. (1978). Structure and function of chicken gizzard myosin. J. Biochem. (Tokyo) *84*, 1529–1542.

Tullio, A.N., Accili, D., Ferrans, V.J., Yu, Z.X., Takeda, K., Grinberg, A., Westphal, H., Preston, Y.A., and Adelstein, R.S. (1997). Nonmuscle myosin II-B is required for normal development of the mouse heart. Proc. Natl. Acad. Sci. USA *94*, 12407–12412.

Watts, F.Z., Shiels, G., and Orr, E. (1987). The yeast MYO1 gene encoding a myosin-like protein required for cell division. EMBO J. *6*, 3499–3505.

Young, P.E., Richman, A.M., Ketchum, A.S., and Keihart, D.P. (1993). Morphogenesis in Drosophila requires nonmuscle myosin heavy chain function. Genes Dev. *7*, 29–41.

Yuste, R., and Bonhoeffer, T. (2001). Morphological changes in dendritic spines associated with long-term synaptic plasticity. Annu. Rev. Neurosci. *24*, 1071–1089.

Zhou, Q., Homma, K., and Poo, M.M. (2004). Shrinkage of dendritic spines associated with long-term depression of hippocampal synapses. Neuron *44*, 749–757.